Simulating an implementation of the surface code in silicon*

Gavin Dold, Sofia Qvarfort, and Simon Schaal
Centre for Doctoral Training in Delivering Quantum Technologies
Department of Physics and Astronomy, University College London
(Dated: June 7, 2016)

We simulate a simple system consisting of one probe qubit and four data qubits as proposed in [**?**] and implement errors such as dephasing, dopant displacement, and path jitter to the full stabiliser measurement cycle.

CONTENTS

I. INTRODUCTION

It is generally agreed upon that large-scale, universal quantum computing will require comprehensive error correction [1, 2].

There has been a recent proposal to make use of dopants in silicon to act as qubits [**?**] to implement a version of the surface code.

We have simulated a probe qubit interacting with four data qubits. The probe qubit is performing a circular orbit 40 nm above the data qubits, and in this document we will document the effect of various errors. These errors include dephasing, dopan placement uncertainties and a path jitter.

A. A physical implementation

In a paper in 2015, it awas proposed by G'Orman *et al.*

Let us first take a closer look at the scheme proposed in [**?**]. The data qubits are dopants placed in silicon placed in a square pattern using the best dopant placement techniques available, which currently stand at [insert some error value and cite it]. To perform the stabiliser measurements, a probe qubit of a different dopant species is placed on a mobile slab above the data qubits. Each probe qubit performs a stabiliser measurement on four data qubits, a procedure which is performed by physically moving the overhead slab with the probe qubits.

Some differences in physical parameters are required.

	T_1	T_2^*	T_2	$T_{2,decoupl}$
P (nat. Si, mK, SET) [3]	0.7 s	55 ns	206 μs	410 μs
P (^{28}Si, mK, SET) [4]		160 μs	1 ms	560 ms
P^{nuc} (^{28}Si, mK, SET) [4]		500 μs	1.75 s	35.6 s
P (^{28}Si, 6.9 K, bulk) [5]			14 ms	
P (^{28}Si, 1.8 K, bulk) [6]			0.6 s	
Bi (^{28}Si, 4.3 K bulk CT) [7]	9 s		2.7 s	
NV (^{12}C, RT) [8, 9]			1.8 ms	3.3 ms
NV (^{12}C, 77 K) [9]				0.6 s
SiC (20 K) [10]		1.1 μs	1.2 ms	
SiC (RT) [11]	185 μs	214 ns	40 μs	

TABLE I: [3, 4]: high field >1T low temp mK. Even good coherenc ebeing close to suurface. [6] supressing instantaneous diffusion. SiC still low collection efficiency. lenses could help. SiC upper bound of 1ms at RT [12] (they have lense). the 1.2ms result has suffered from low collection efficiency

II. SPIN SPECIES

Donors deep in bulk show longer coherence times $T_2^e = 2$ s [6] not applicable for us.

III. THE SIMULATION

In this section, we will describe how we go about simulating the interaction between the probe qubit and the data qubit. The interaction is governed by the following Hamiltonian:

$$H = \mu_B B(g_1\sigma_1^Z + g_2\sigma_2^Z) + \frac{J}{r^3}(\sigma_\mathbf{1}\cdot\sigma_\mathbf{2} - 3(\hat{\mathbf{r}}\cdot\sigma_\mathbf{1})(\hat{\mathbf{r}}\cdot\sigma_\mathbf{2})) \quad (1)$$

The effect of this Hamiltonian is to evolve the probe qubit in a particular direction depending on the state of the data qubit. By initialising the probe qubit in the $|+\rangle$

* The authors would like to thank Dan Browne and John Morton for fruitful discussions.

state, the final parity measurement will entail finding the probe qubit in either the $|+\rangle$ state (even parity) or in the $|-\rangle$ state. This can be understood by the fact that each data qubit imparts a $\frac{\pi}{2}$ phase in

A. Finding the correct evolution time

The speed of the simulation is set by the total time it takes to complete one full cycle. We want the accumulated phase for an even parity measurement to reach 2π exactly. The plot in Figure **??** shows the accumulated phase as a function of evolution time.

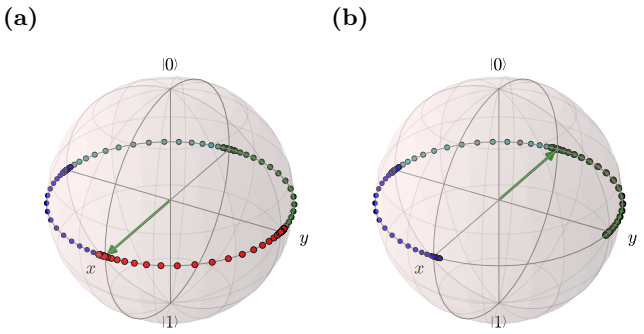

FIG. 1

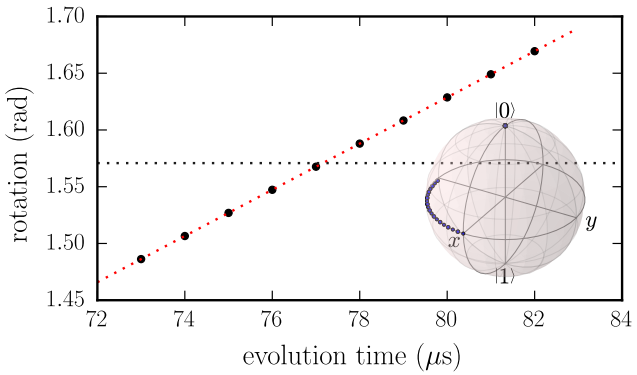

FIG. 2

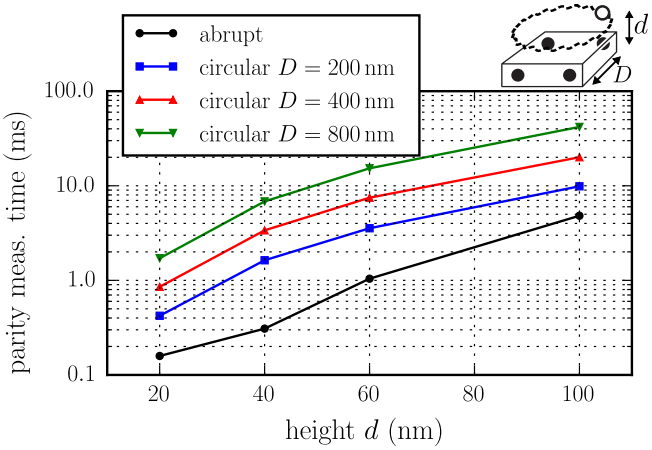

FIG. 3

IV. ERRORS

In this section, we will detail the results that o

A. Path Jitter

The final error that we introduce and simulate is jitter in the path taken by the probe qubits. The precision provided by modern MEMS control structures is about 1 nm [**?**],

It was found that adding just a random jitter to the path introduced jumps which the solver could not handle very well. Instead, we overlay a sinusoidal motion over the circular motion, effectively causing a periodic deviation from the perfect path. We introduced a random element in the starting phase and amplitude [check this!]

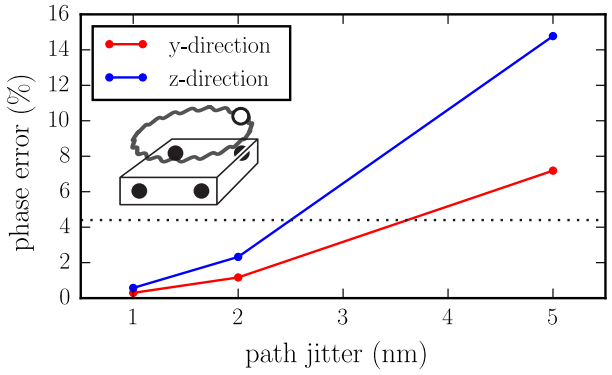

FIG. 4

B. Dephasing

In this section, we present results from simulations of the Lindblad master equation where a dephasing channel

is turned on. This channel contains the Lindblad operator

$$L = \sqrt{\Gamma}\sigma_z \tag{2}$$

where Γ is the dephasing parameter. Γ can also be written as $1/\tau$ where τ is the dephasing time. We evolve the system under the Lindblad master equation for an odd number of errors. In this simulation, the error is a bit-flip error on the fourth data qubit. As a result, the probe qubit 'backtracks' during the last quarter of the run such that its final phase ends up at $\phi = \pi$.

In Figure 6, we see the effect of a small dephasing coefficient (100) whereas in Figure 7 we see the effect of larger dephasing (500). Note that the dephasing happens primarily as the interaction between the probe qubit and the data qubit is weak, where the phase of the probe qubit doesn't evolve.

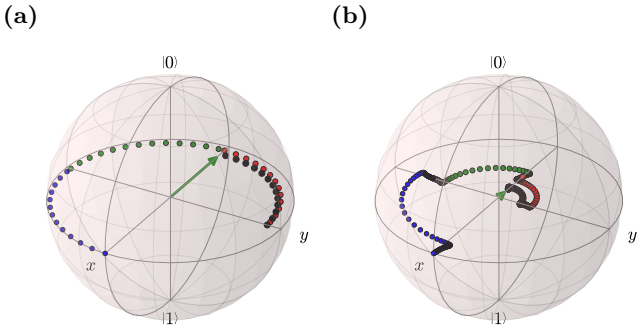

FIG. 5

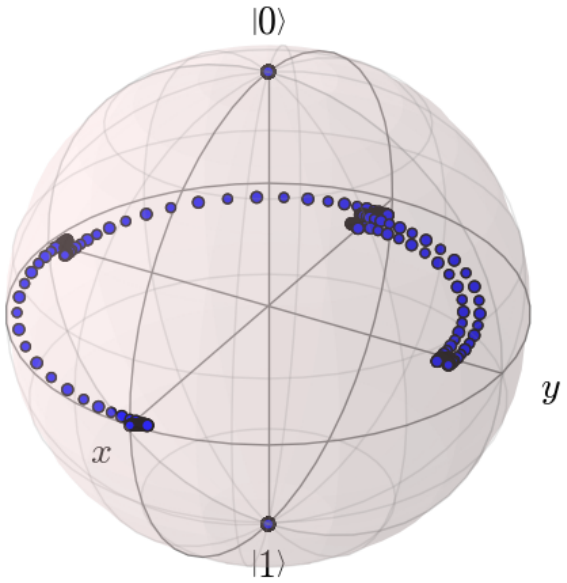

FIG. 6: The states of the probe and data qubits plotted in the Bloch sphere with a dephasing parameter of 100, which translates to a dephasing time of 10 ms. The phase of the probe qubit is not affected since no relaxation or excitation is taking place. The effect can however be seen in the probability of measuring the probe qubit in the $|+\rangle$ or $|-\rangle$ state. For complete dephasing, the probe qubit will become the maximally mixed state and the measurement outcomes are completely random. The states of the probe and data qubits plotted in the Bloch sphere with a dephasing parameter of 100, which translates to a dephasing time of 10 ms.

In Figure 8 we see the effect of dephasing on the probability of measuring the correct value of the probe qubit. Since there is an odd number of errors, we want the probe qubit to end up in the $|-\rangle$ state. However, the dephasing will cause the probe qubit to become a mixed state ρ, which means that there is a non-zero probability of measuring $|+\rangle$ instead of $|-\rangle$. For complete dephasing, the probe qubit becomes a mixed state which has a 50–50% chance of measuring either state.

In Figure 8, we have market the data-point for dephasing corresponding to the decoherence time for Bismuth, which is one of the proposed donor types for the probe qubit. The decoherence time of bismuth is 2.7 s [7], which leads to a dephasing parameter of $0.37\,\mathrm{s}^{-1}$.

It should be noted that the Bismuth dephasing time of 2.7 s can only be obtained by applying advanced Hahn echo readout methods. Whereas it is cumbersome, this technique is not beyond the capabilities of modern experiments.

C. Data qubit displacement

The proposal [13] as described in section I A utilises two distinct qubit arrays each of lattice constant D, separated by a distance d perpendicular to the planes. To achieve reasonable interaction times compared to qubit decoherence times, distances $D = 400\,\mathrm{nm}$ and $d = 40\,\mathrm{nm}$ have been chosen for simulation.

It is may prove unrealistic, however, to expect to be able to deterministically place qubits with nm precision in a scalable manner. Resolutions of 10 nm can be achieved using e-beam lithography [**?**] or nanostencil masks [14], combined with single-ion implantation techniques [15]. STM patterning techniques offer atomic precision of dopants in Si [16] but a method of maintaining this precision over an array several µm across remains elusive.

To consider in detail the effect of these displacements, we generated uniformly random offsets to the position of each data qubit within a pillbox of heigh and radius R, as illustrated in fig. 9a. This form of displacement is the same as used in the proposal [13] and was chosen as the displacement in the x–y plane would be expected to be uniformly radial, and the implantation depth in the z-axis would be independent from this.

To illustrate the errors qubit displacement creates, consider a set of typical qubit displacements as illustrated in fig. 9b. These displacements give each data qubit a different distance r at which it is closest to the probe qubit as it passes overhead, resulting in a different interaction strength. Hence the phase accumulated for each data

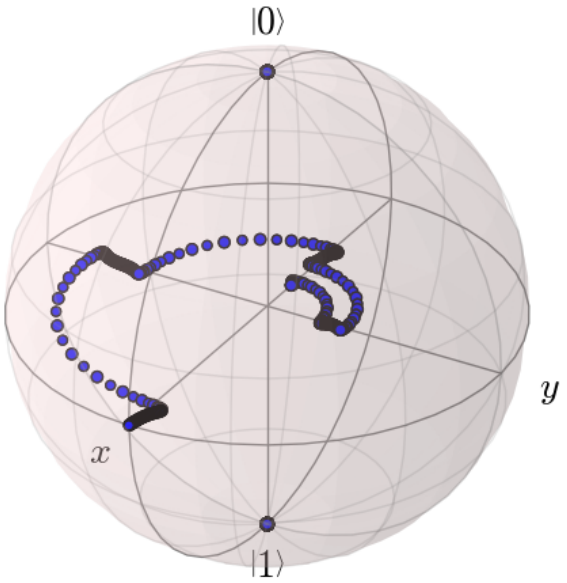

FIG. 7: The states of the probe and data qubits plotted in the Bloch sphere with a dephasing parameter of 500, which translates to a dephasing time of 2 ms. The strong dephasing causes the probe qubit state to drift quickly towards the maximally mixed state.

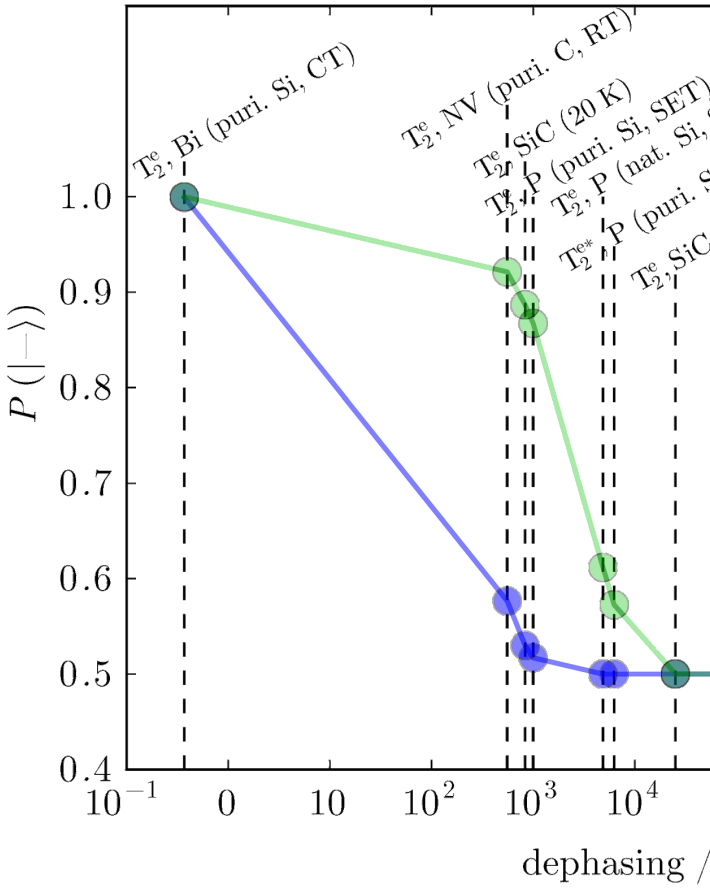

FIG. 8: A graph showing the relationship between the dephasing parameter Γ and the probability $P(|-\rangle)$ of measuring the probe qubit in the $|-\rangle$ state. In this simulation, one of the data qubits have undergone a bit-flip error. As the dephasing parameter increases, the probe qubit moves towards the maximally mixed state and the probability of measuring $|-\rangle$ goes towards 0.5. The dephasing parameter for Bismuth as a material for the probe qubit has been market in the graph.

qubit varies from the ideal $\frac{\pi}{2}$ by an independent amount. These errors are systematic in that the same phases are picked up for each parity measurement, unlike the probe jitter considered in section IV A.

We find that for these displacements, the case of even parity (no bit-flips) yields close to a 2π evolution with 99.968% probability of successfully measuring $|+\rangle$, from the evolution shown in fig. 9c. However, on introducing bit-flip errors to each of the four data qubits, different phase accumulations are observed as in fig. 9d.

[FIND A GOOD SPOT TO INSERT THIS LATER] This was considered in the proposal [13], and using a simulation of the logical surface code operations a threshold of 6.1 nm was derived.

[BELOW LIES OLD CRAP]

The effect of displacement of the data qubits from the ideal was investigated. Ideally the data qubits would be in a square lattice of spins precisely $D = 400$ nm apart, but due to inaccuracies in dopant spin placement each qubit will have small displacements from the ideal lattice position.

This is modelled by generating a uniform random displacement within a given pillbox xy-radius and z-height. Simulations from the original paper show radius = height = 6 nm to be a threshold for this scheme. The phase accumulated over 25 runs for this pillbox size is plotted as a histogram in fig. **??**, showing a maximum phase error of $\frac{\pi}{4}$ for these runs.

The effect of displacements in the x-y plane and the z-axis are significantly different in magnitudes, due to the $\frac{1}{d^3}$ term in the Hamiltonian being most strongly affected by z displacements. This effect was investigated by artificially setting displacements in these directions.

Fig. **??** shows changes in accumulated phase due to z-displacements. The first 2 qubits are displaced 4 nm down, slowing the evolution and giving a noticeable phase error after half a cycle. However, qubit 4 is displaced 3 nm upwards, reducing d and resulting in faster evolution. The effect is a small phase error from the ideal 2π.

Fig. **??** shows the effect of displacements in the x-y plane. For this run, all data qubits were displaced 10 nm inwards with respect to the circular motion. The phase

error on each individual qubit is then less than that produced by the 3 nm z-displacement of fig. **??**, showing the smaller sensitivity to displacement in the x-y plane, though the overall error after all 4 qubits is greater as in the z-direction, $+z$ and $-z$ errors cancel out somewhat, whereas xy displacement errors will always slow the evolution.

1. *Twirling*

It is not the fact that the resultant success probabilities are lower than the even parity case that is especially concerning; this is what fault-tolerant codes are designed to cope with. Instead it is the fact that bit-flips on each qubit give a *different* probability of successful detection. This means one qubit will me more prone to undetected errors than others. The fault tolerance required by the proposal assumes a symmetry between the data qubits that this breaks, making the code susceptible to logical errors.

V. CONCLUSIONS AND OUTLOOK

In this report, we have presented the results obtained from simulating the interaction between one probe qubit and four data qubits as in the proposed scheme in [**?**].

[1] D. S. Wang, A. G. Fowler, and L. C. L. Hollenberg, Physical Review A - Atomic, Molecular, and Optical Physics **83**, 020302 (2011), arXiv:1009.3686 [quant-ph].

[2] A. G. Fowler, M. Mariantoni, J. M. Martinis, and A. N. Cleland, Physical Review A - Atomic, Molecular, and Optical Physics **86** (2012), 10.1103/PhysRevA.86.032324, arXiv:1208.0928.

[3] J. J. Pla, K. Y. Tan, J. P. Dehollain, W. H. Lim, J. J. L. Morton, D. N. Jamieson, A. S. Dzurak, and A. Morello, Nature **489**, 541 (2012), arXiv:1305.4481.

[4] J. T. Muhonen, J. P. Dehollain, A. Laucht, F. E. Hudson, T. Sekiguchi, K. M. Itoh, D. N. Jamieson, J. C. McCallum, A. S. Dzurak, and A. Morello, ArXiv **9**, 1 (2014), arXiv:1402.7140.

[5] G. W. Morley, M. Warner, a. M. Stoneham, P. T. Greenland, J. Van Tol, C. W. M. Kay, and G. Aeppli, Society **9**, 19 (2010).

[6] A. M. Tyryshkin, S. Tojo, J. J. L. Morton, H. Riemann, N. V. Abrosimov, P. Becker, H.-j. Pohl, T. Schenkel, M. L. W. Thewalt, K. M. Itoh, and S. A. Lyon, Nature Materials **11**, 18 (2011), arXiv:1105.3772.

[7] G. Wolfowicz, A. M. Tyryshkin, R. E. George, H. Riemann, N. V. Abrosimov, P. Becker, H.-J. Pohl, M. L. W. Thewalt, S. a. Lyon, and J. J. L. Morton, Nature nanotechnology **8**, 561 (2013), arXiv:1301.6567.

[8] G. Balasubramanian, P. Neumann, D. Twitchen, M. Markham, R. Kolesov, N. Mizuochi, J. Isoya, J. Achard, J. Beck, J. Tissler, V. Jacques, P. R. Hemmer, F. Jelezko, and J. Wrachtrup, Nature materials **8**, 383 (2009).

[9] N. Bar-Gill, L. M. Pham, A. Jarmola, D. Budker, and R. L. Walsworth, Nature communications **4**, 1743 (2013), arXiv:arXiv:1211.7094v2.

[10] D. Christle, A. Falk, and P. Andrich, arXiv **14**, 25 (2014), arXiv:1406.7325.

[11] W. F. Koehl, B. B. Buckley, F. J. Heremans, G. Calusine, and D. D. Awschalom, Nature **479**, 84 (2011).

[12] M. Widmann, S.-Y. Lee, T. Rendler, N. T. Son, H. Fedder, S. Paik, L.-P. Yang, N. Zhao, S. Yang, I. Booker, A. Denisenko, M. Jamali, S. A. Momenzadeh, I. Gerhardt, T. Ohshima, A. Gali, E. Janzén, and J. Wrachtrup, Nature materials **14**, 1 (2014), arXiv:1407.0180.

[13] J. O'Gorman, N. H. Nickerson, P. Ross, J. J. Morton, and S. C. Benjamin, npj Quantum Information **2**, 15019 (2016).

[14] C. D. Weis, A. Schuh, A. Batra, A. Persaud, I. W. Rangelow, J. Bokor, C. C. Lo, S. Cabrini, E. Sideras-Haddad, G. D. Fuchs, R. Hanson, D. D. Awschalom, and T. Schenkel, Journal of Vacuum Science & Technology A: Vacuum, Surfaces, and Films **26**, 2596 (2008), arXiv:0806.2167.

[15] D. N. Jamieson, C. Yang, T. Hopf, S. M. Hearne, C. I. Pakes, S. Prawer, M. Mitic, E. Gauja, S. E. Andresen, F. E. Hudson, A. S. Dzurak, and R. G. Clark, Applied Physics Letters **86**, 1 (2005).

[16] S. R. Schofield, N. J. Curson, M. Y. Simmons, F. J. Ruess, T. Hallam, L. Oberbeck, and R. G. Clark, Physical review letters **91**, 136104 (2003), arXiv:0307599 [cond-mat].

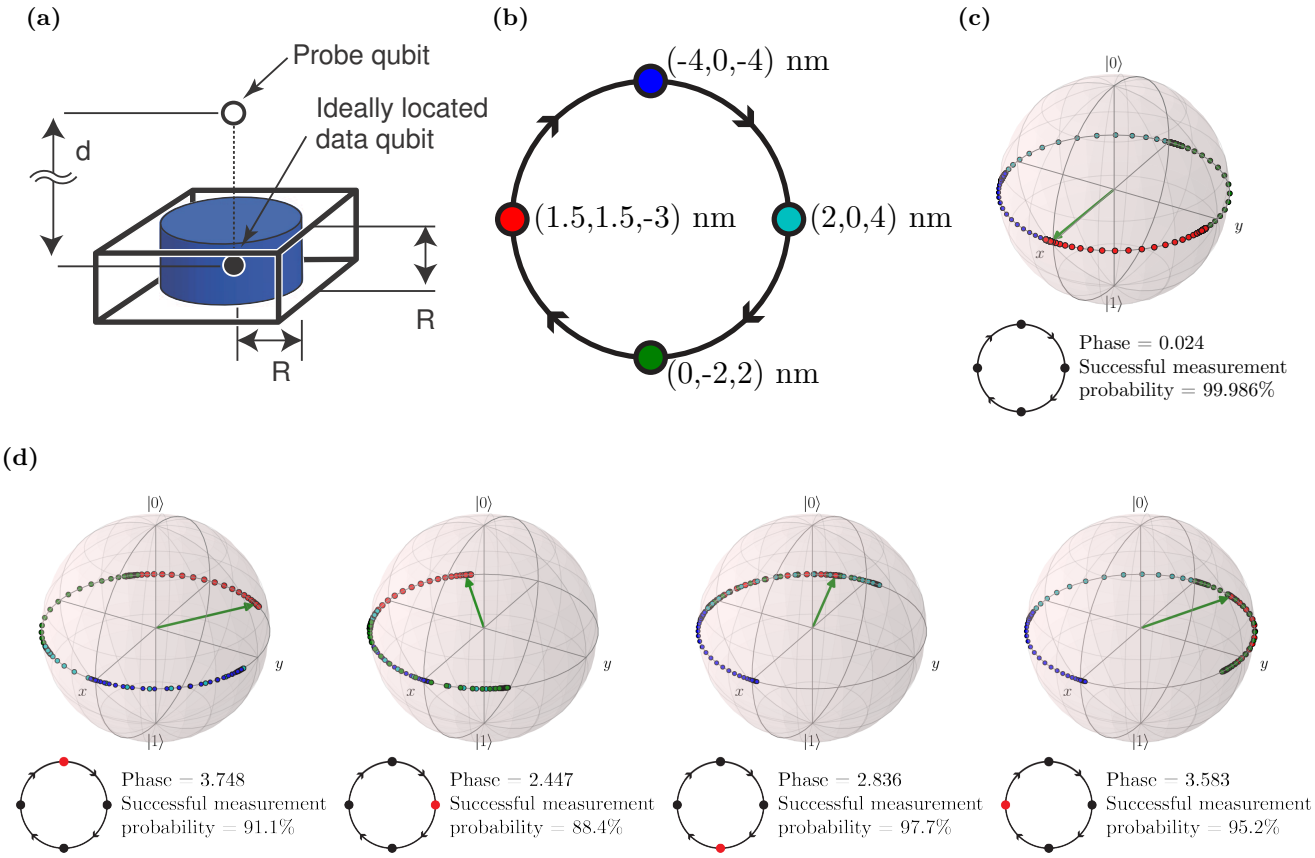

FIG. 9: aoeu NOTE: change last subfigure to .pdf

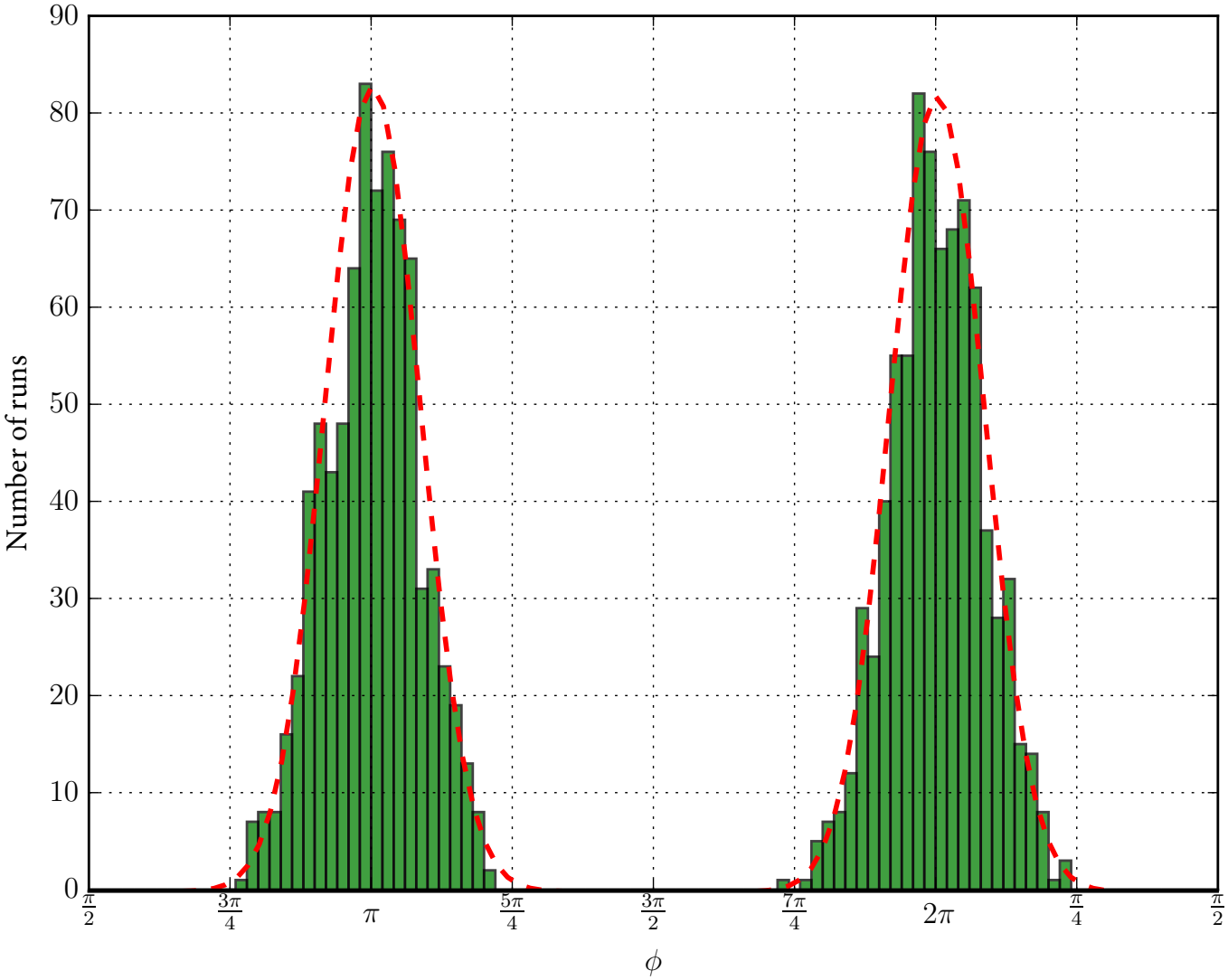

FIG. 10: Phase errors over 25 runs as a result of randomly generated data qubit displacements within a pillbox of half-height 3 nm and radius 6 nm. These values are a threshold for the proposed scheme.